Measurement of the 477.6-keV γ-ray production cross section following inelastic neutron scattering by ^{7}Li

M. Nyman,[1,*] F. Belloni,[1] D. Ichinkhorloo,[2] E. Pirovano,[1] A. J. M. Plompen,[1] and C. Rouki[1]
[1]*European Commission, Joint Research Centre, Institute for Reference Materials and Measurements, Retieseweg 111, B-2440 Geel, Belgium*
[2]*Meme Media Laboratory, Hokkaido University, Sapporo 060-8628, Japan*
(Received 8 December 2015; published 19 February 2016)

The γ-ray production cross section for the 477.6-keV $1/2^- \rightarrow 3/2^-_{\text{g.s.}}$ transition in ^{7}Li following inelastic neutron scattering has been measured from the reaction threshold up to 18 MeV. This cross section is interesting as a possible standard for other γ-ray production cross-section measurements. The experiment was conducted at the GELINA pulsed white neutron source with the GAINS spectrometer consisting of 12 high-purity germanium detectors. The time-of-flight method was used for neutron energy determination. The sample was an optical-quality lithium fluoride disk and the neutron flux was monitored using a ^{235}U fission chamber. Previous measurements of this cross section are reviewed and compared with our results. Recently, the examined cross section has been calculated using the continuum-discretized coupled-channels method. The results are found to be in reasonable agreement with the experimental data.

DOI: 10.1103/PhysRevC.93.024610

I. INTRODUCTION

In experiments involving neutron beams, the flux is often measured with a transmission fission chamber, containing, e.g., ^{235}U, ^{238}U, or ^{239}Pu. The disadvantage of such a system is the low counting rate of the fission events, which necessitates long acquisition times for collecting adequate statistics. A sample pulse-height spectrum from the fission chamber used in this work is shown in Fig. 1. An alternative method for neutron fluence determination could be the measurement of γ rays following inelastic scattering, provided that the γ-ray production cross section is known sufficiently well. Several possibilities for a reference cross section have been considered in [1,2], where the 477.6-keV $1/2^- \rightarrow 3/2^-_{\text{g.s.}}$ transition in ^{7}Li was concluded to be one of the best candidates. Factors making this transition favorable include an isotropic γ-ray emission, a negligible internal conversion coefficient, a low inelastic threshold (546 keV), and a fairly smooth energy dependence of the cross section.

Lithium and beryllium fluorides are also interesting as coolants for molten salt reactor systems, as described in the Technology roadmap for generation IV nuclear energy systems [3]. Additionally, in deuterium-tritium fusion reactors the fuel cycle requires breeding of tritium from ^{6,7}Li. The interactions between neutrons and lithium affect the tritium breeding ratio, nuclear heating, and radiation damage. Thus good quality nuclear data on neutron- and proton-induced reactions of ^{6,7}Li are necessary.

The inelastic neutron scattering cross section to the first excited state in ^{7}Li was first reported by Freeman *et al.* in 1955 from the threshold to neutron energy $E_n = 1.65$ MeV [4]. Since then, the $^7\text{Li}(n,n'\gamma)^7\text{Li}^*$(477.6 keV) cross section has been measured in several experiments, which are summarized in Table I. The early γ-ray measurements by Freeman *et al.*, Bostrom *et al.* [5], and Benveniste *et al.* [6] were performed using scintillation detectors and a ring scatterer. More information about the experimental setup by Benveniste *et al.* is provided in Refs. [7,8].

These measurements were followed by several others where, instead of γ-ray detection, the scattered neutrons were observed [9–12]. With the exception of the experiment of Glazkov [9], all of them used scintillator detectors and were normalized with the known H(n,n)H cross section. These data sets tend to contain a small number of measurement points, typically with large uncertainty margins. They also do not extend above 5 MeV in neutron energy. In addition to the references mentioned above, the experimental methods are discussed in [13–16].

The vast majority of $^7\text{Li}(n,n'\gamma)^7\text{Li}^*$(477.6 keV) cross section data originates from experiments conducted in the 1970s. These cover a neutron energy range from the threshold up to 21 MeV. In three of these experiments, by Presser and Bass [17], Smith [18], and Olsen *et al.* [19], lithium-drifted germanium [Ge(Li)] detectors were used for detecting the γ rays. All three experiments used different reactions for neutron production and different methods for determining the neutron flux. Additional information on the experimental setup used by Smith is available in [20–22]. The proton-recoil telescope used by Olsen *et al.* for neutron flux measurement is described in [23]. The data sets by Dickens *et al.* [24] and Morgan [25] from Oak Ridge National Laboratory, obtained from γ-ray measurements using scintillator detectors, are by far the most comprehensive data sets available, extending from the inelastic threshold up to approximately 20 MeV. In both cases, an electron linac white neutron source and the time-of-flight method for neutron energy determination were used. More details about the experimental system used in these experiments can be found in [26]. Finally, there is one data point from a γ-ray measurement at $E_n = 14$ MeV by Besotosnyj *et al.* [27] and five points between $2.6 < E_n < 4.6$ MeV by Knox *et al.* [28]. In the latter case, Ref. [28] is

*markus.e.j.nyman@gmail.com

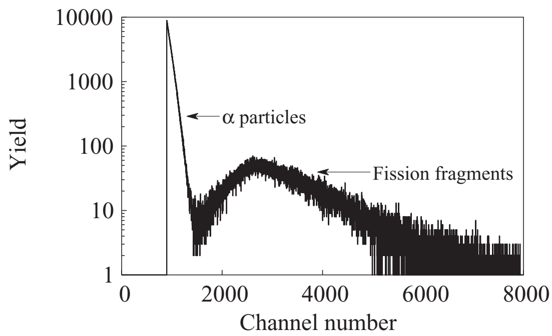

FIG. 1. A sample pulse-height spectrum of events observed in the Institute for Reference Materials and Measurements (IRMM) fission chamber in the 200-m experiment (see Sec. II for details). The spectrum corresponds to approximately 15 days of measurement time with an average neutron flux of 270 s^{-1} cm^{-2}.

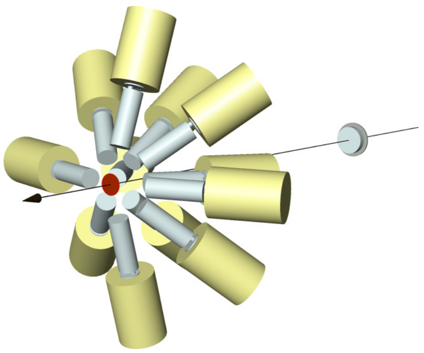

FIG. 2. A schematic representation of the GAINS array, modeled using the SimpleGeo software [37]. The direction of the neutron beam is indicated with the arrow. The ^{235}U fission chamber can be seen behind the HPGe-detector array.

cited in the EXFOR database [29], although the experimental data does not not appear in the article. The reference given in Table I, [30], includes a description of the experimental setup. Finally, the same group reported measurements of the integrated cross section for inelastic neutron scattering to the first excited state in ^{7}Li from $E_n = 4$ to 7.5 MeV [31]. These data are not included in the EXFOR database.

The cross section for the $^7\mathrm{Li}(n,n'\gamma)^7\mathrm{Li}^*$(477.6 keV) reaction has been evaluated extensively by R-matrix calculations, e.g., [28,32,33]. A good agreement with experimental data has been achieved. The continuum-discretized coupled-channels method (CDCC) [34,35] has been successful in describing breakup processes of weakly bound light nuclei. For $n + {}^7$Li reactions these have thresholds of approximately $E_n = 2.8$ MeV or higher. Recent CDCC calculations will be compared to our experimental results in Sec. IV B.

As the existing data consists of multiple sets which are not always consistent with each other, remeasuring this cross section is important. This is especially true if it is intended to be used as a standard. Furthermore, the total relative uncertainty of the cross section should be made as small as possible, preferably below 5%. The Gamma array for inelastic neutron scattering (GAINS) spectrometer [36] was developed for high-precision cross-section measurements of $(n,xn\gamma)$ reactions at the Geel electron linear accelerator (GELINA) time-of-flight facility. The high γ-ray detection efficiency and energy resolution of GAINS, together with a very good time resolution, allows γ-ray production cross sections to be measured to the desired level of uncertainty.

II. EXPERIMENTAL SETUP

Two measurements were conducted at the IRMM in 2015. The neutrons were produced using the GELINA pulsed white neutron source with an 800-Hz repetition rate, and the GAINS spectrometer was used for γ-ray detection. Currently, GAINS consists of 12 large-volume high-purity germanium (HPGe) detectors manufactured by CANBERRA, mounted at 110°, 125°, and 150° with respect to the beam direction, with four detectors at each angle. A schematic of the array is presented in Fig. 2. For the first measurement GAINS was located at the GELINA flight path 3, and the sample was positioned at 198.757(5) m from the neutron source. In May 2015, in preparation for future experiments, the setup was repositioned at the same flight path with the sample at 99.676(5) m from the neutron source. The detectors were mounted in a new support frame, maintaining the same geometry and without changing any of the associated electronics. ^{7}Li data was collected as a test experiment. Hereafter these will be referred to as the 200-m and 100-m measurements. The neutron flux was measured with a ^{235}U fission chamber located at 146.8 or 211.5 cm upstream from the GAINS sample position in the 200- or 100-m measurements, respectively. The chamber contains 8 UF_4 deposits of 70 mm diameter, placed on five aluminum foils (20 μm thickness). Details on the chamber are presented in [38,39]. The data acquisition system for the HPGe detectors uses Acquiris DC440 digitizers, which have a 12-bit amplitude resolution and a sampling rate of 440 million samples/s. A more detailed description of the data acquisition system is provided in [40]. The sample was an optical-quality lithium fluoride (LiF) disk supplied by Te Lintelo Systems. The abundance of ^{7}Li in natural lithium is 92.41(4)% [41]. The physical properties of the sample, determined by measurements performed at the IRMM, are summarized in Table II. The sample area was measured with a Mitutoyo Quickscope vision measuring machine, the mass with a Mettler Toledo PG603-S balance, and the thickness with a vernier caliper.

III. DATA ANALYSIS

The procedure for extracting γ-production, level population, and inelastic scattering cross sections from GAINS data is described in [36,38,39]. The points relevant to this discussion will briefly be reviewed here. Experimentally, the determination of the γ-ray production cross section starts from the measured differential γ-production cross section $d\sigma_i/d\Omega$. At neutron energy E_n for detector i positioned at an angle θ_i this is given by

$$\frac{d\sigma_i}{d\Omega}(\theta_i,E_n) = \frac{1}{4\pi}\frac{Y_i(E_n)}{Y_{\mathrm{fc}}(E_n)}\frac{\epsilon_{\mathrm{fc}}\sigma_{\mathrm{U}}(E_n)}{\epsilon_i}\frac{t_{\mathrm{U}}}{t_{\mathrm{s}}}\frac{A_{\mathrm{s}}}{A_{\mathrm{U}}}\frac{1}{c_{\mathrm{ms}}(E_n)}, \quad (1)$$

TABLE I. Previous measurements of the γ-ray production cross section for the 477.6-keV $1/2^- \rightarrow 3/2^-_{\mathrm{g.s.}}$ transition in ^{7}Li. The time-of-flight method used for background suppression or neutron energy measurement is indicated by the acronym TOF. Other abbreviations used in the table are αPM (α-particle monitoring), LS (liquid scintillator), PS (plastic scintillator), PHD (pulse-height discrimination), PSD (pulse-shape discrimination), and geom. (geometry). The institutes are AERE (Atomic Energy Research Establishment, Harwell), ANL (Argonne National Laboratory, Argonne), AWRE (Atomic Weapons Research Establishment, Aldermaston), CBNM (Central Bureau for Nuclear Measurements, Geel; currently IRMM), IAE (I.V. Kurchatov Institute of Atomic Energy, Moscow), KIT (Karlsruhe Institute of Technology, Karlsruhe), LANL (Los Alamos National Laboratory, Los Alamos), LLNL (Lawrence Livermore National Laboratory, Livermore), and ORNL (Oak Ridge National Laboratory, Oak Ridge).

Authors and Institute	Year	E_n range (MeV)	Neutron production	Data points	Detected particle	Detectors	Neutron flux measurement	Comments	Ref.
Freeman *et al.* AERE	1955	0.415–1.645	$T(p,n)^3$He	44	γ	NaI, stilbene	BF_3 monitor + calibrated BF_3 detector	Ring geom.	[4]
Bostrom *et al.* Texas Nuclear Corp.	1959	1.01	N/A	1	γ	NaI(Tl)	N/A	Ring geom.	[5]
Benveniste *et al.* LLNL	1962	13.57–14.75	$T(d,n)^4$He	12	γ	NaI	αPM	Ring geom. TOF	[6]
Glazkov Obninsk Power-Physics Institute	1963	0.8–1.2	$T(p,n)^3$He	2	n	^{3}He	Absolute measurement	Inverse spherical geom.	[9]
Batchelor and Towle AWRE	1963	1.5–4.0	$T(p,n)^3$He	3	n	LS	H(n,n)H	TOF	[10]
Hopkins *et al.* LANL	1968	3.35–4.83	$T(p,n)^3$He	2	n, γ	NaI(Tl), NE102A PS	H(n,n)H	TOF	[11]
Knitter and Coppola CBNM	1968	1.12–2.30	$T(p,n)^3$He	8	n	NE102A PS	H(n,n)H	TOF	[12]
Presser and Bass KIT	1972	0.95–8.8, 19–21	$T(p,n)^3$He $D(d,n)^3$He $T(d,n)^4$He	187	γ	Ge(Li)	PS (absolute n-flux measurement)	$\pm$15% uncertainty in absolute scale	[17]
Besotosnyj *et al.* IAE	1975	14	$T(d,n)^4$He	1	γ	NaI	Absolute measurement	TOF	[27]
Smith ANL	1976	0.57–4	^{7}Li$(p,n)^7$Be	70	γ	Ge(Li)	^{235}U(n,F)	TOF	[18]
Dickens *et al.* ORNL	1977	0.538–20.57	$e^- +$ Ta	285	γ	NaI	NE-110 PS NE-213 LS PS monitor	TOF, PHD	[24]
Morgan ORNL	1978	0.5004–19.83	$e^- +$ Be	405	γ	NE-213 LS	PS monitor NE-213 LS	Ring geom. TOF, PSD	[25]
Knox *et al.* Ohio University	1979	2.6–4.6	$T(d,n)^4$He	5	n	NE-224 LS	NE-224 LS	TOF	[30]
Olsen *et al.* ORNL	1980	0.5–5.0	$e^- +$ Ta	43	γ	Ge(Li)	H(n,n)H (p-recoil telescope)	TOF	[19]

where $Y_i(E_n)$ is the γ-ray yield, $Y_{\mathrm{fc}}(E_n)$ the fission chamber yield, ϵ_{fc} the fission chamber efficiency, ϵ_i the γ-ray detection efficiency, $\sigma_{\mathrm{U}}(E_n)$ the cross section of the ^{235}U(n,F) reaction from [42], and t_{U}, t_{s}, A_{U}, A_{s} the mass areal densities and atomic masses, respectively, of ^{235}U in the fission chamber, and the sample under study. The values used here were $t_{\mathrm{U}} = 0.003084(7)$, $t_{\mathrm{s}} = 0.13377(8)$ g/cm^2, $A_{\mathrm{U}} = 235.0439299(20)$ [43], and $A_{\mathrm{s}} = 7.0160034256(45)$ u [44]. Finally, $c_{\mathrm{ms}}(E_n)$ is the correction factor for multiple neutron scattering, determined from Monte Carlo simulations (see below). The diameters of the sample and the ^{235}U deposits in the fission chamber were larger than that of the neutron beam. This is beneficial because Eq. (1) does not need to account for the fraction of the beam intercepting the ^{235}U deposits or the sample. However, the homogeneity of the sample and the

TABLE II. Physical properties of the LiF sample. The density was calculated from the measured values; the density stated by the supplier of the disk is 2.64 g/cm^3.

Area (mm^2)	5022.62(8)
Diameter (mm)	79.971(1)
Thickness (mm)	2.05(1)
Mass (g)	27.17(1)
Density (g/cm^3)	2.645(13)

deposits is important. In the present case there was no issue with the homogeneity of the LiF disk. For the fission chamber a correction for inhomogeneity was applied, as described in [39].

Integrating the differential cross sections is particularly simple in the case of the $1/2^- \to 3/2^-_{\text{g.s.}}$ transition in ^{7}Li, as the γ-ray emission is isotropic. Thus, the differential cross section from any given detector needs only to be multiplied by a factor of 4π to obtain the total γ-ray production cross section σ_γ. This was verified in our experiment by the observation that cross sections obtained from detectors at different angles were consistent with each other.

The neutron energy E_n corresponding to a given time-of-flight bin was calculated in the following manner:

$$E_n = E_0\left[\frac{1}{\sqrt{1-\left(\frac{L}{ct}\right)^2}} - 1\right], \quad (2)$$

where E_0 is the rest mass of the neutron, L is the neutron flight path length, c is the speed of light in vacuum, and t is the neutron time-of-flight.

The determination of the absolute γ-ray detection efficiency of the GAINS spectrometer relies on Monte Carlo simulations described in [45]. First, the absolute γ-ray detection efficiency is determined experimentally with a ^{152}Eu point source. An MCNP5 [46] simulation is then performed and the model of the setup is adjusted until a satisfactory agreement between the experimental and simulated efficiencies is achieved. The final efficiencies are then determined by using the optimal detector geometry in a simulation in which the point source is replaced with a volume source corresponding to the size and material of the sample.

The procedure followed here to determine the fission chamber efficiency is described in [39]. Corrections were also applied to account for neutron flux attenuation between the fission chamber and the sample and multiple neutron scattering in the sample itself. These were evaluated by comparing MCNP5 simulations of the actual experimental setup and of the same configuration with the sample and all materials between the fission chamber and the sample removed. The resulting correction coefficient c_{ms} as a function of neutron energy is shown in Fig. 3. As can be seen from the figure, the correction for such a thin sample is fairly small.

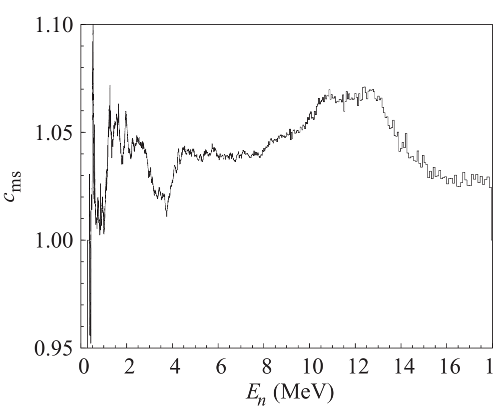

FIG. 3. The multiple-scattering correction coefficient c_{ms} determined for the experimental setup at flight path 3 200 m, as a function of neutron energy.

IV. RESULTS AND DISCUSSION

A. Experimental data

In the case of ^{7}Li the only observed γ ray originates from the 477.6-keV transition from the first excited state to the ground state. A sample γ spectrum covering the region of interest is shown in Fig. 4. As can be seen from the figure, the 477.6-keV peak from ^{7}Li is shifted and broadened owing to the Doppler effect. The second excited level in ^{7}Li lies at 4 630 keV and decays into $\alpha + t$. It is therefore not observed in the present experiment. All the higher excited states of ^{7}Li are also unstable against particle emission. The most prominent peak in Fig. 4 comes from the 197.1-keV transition from the second excited level to the ground state in ^{19}F. This peak, which is not fully visible in Fig. 4, contains more than six times the number of counts as the 477.6-keV one. This γ ray was not included in the analysis because the second excited state in ^{19}F has a half-life of 89.3(10) ns [47], making it difficult to apply the time-of-flight method.

The time resolution achieved with the GAINS setup is approximately 10 ns. For a 200-m flight path this corresponds to a neutron energy resolution of 1.4 keV for $E_n = 1$ MeV, increasing to 44 keV for $E_n = 10$ MeV. Both IRMM data sets meet the goal of the total relative uncertainty being less than 5% for most of the measurement points. With $1 < E_n < 8$ MeV, the average relative uncertainty is approximately 4.5% for both experiments. The main components of the total uncertainty are the HPGe detector efficiency calibration, the fission chamber efficiency, the ^{235}U(n,F) cross section, and statistical uncertainties of the γ-ray and fission chamber yields.

The γ-ray production cross section for the 477.6-keV transition in ^{7}Li is displayed in Fig. 5 along with previous experimental data from [4,5,9–12,17–19,24,25,28]. For clarity,

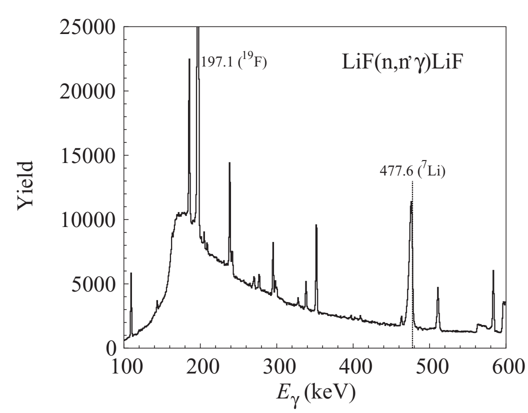

FIG. 4. A sample γ-ray spectrum from the reaction LiF(n,$n'\gamma$)LiF. The two peaks originating from ^{7}Li and ^{19}F are labeled with their energies. The other peaks are from the ambient background. The ^{7}Li peak is broadened and shifted owing to the Doppler effect (the 477.6-keV position is indicated with a dashed line). The detector from which the spectrum was obtained was located at an angle of 150° with respect to the beam direction.

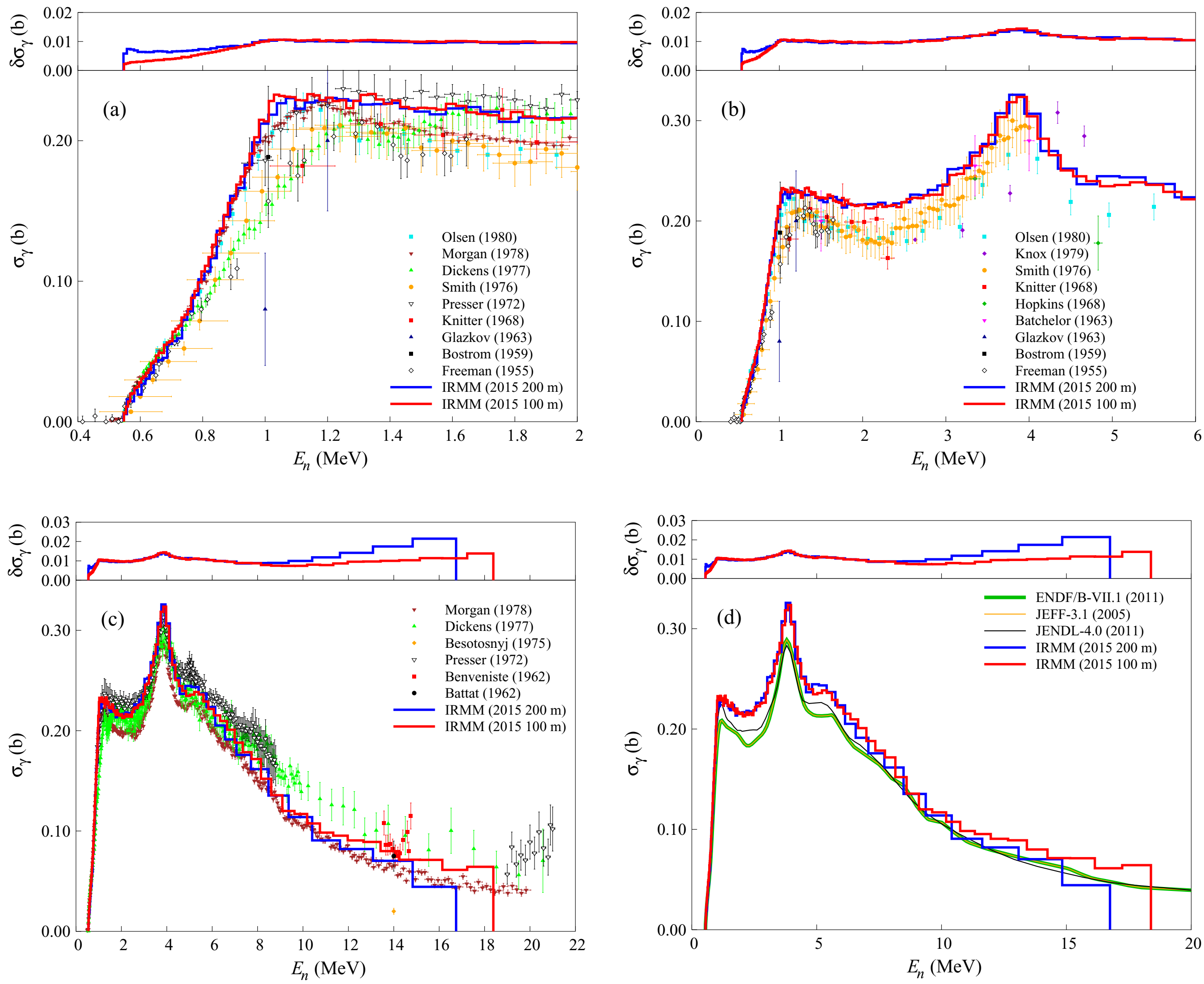

FIG. 5. The γ-ray production cross section σ_γ for the 477.6-keV transition in ^{7}Li, measured using the reaction LiF($n,n'\gamma$)LiF, compared to other experimental data and three nuclear data evaluations. (a) The cross section from the threshold to $E_n = 2$ MeV. (b) Comparison up to $E_n = 6$ MeV. (c) Our results compared to data sets that cover high neutron energies. (d) The IRMM measurements compared to the evaluated cross sections from the ENDF/B-VII.1, JEFF-3.1, and JENDL-4.0 libraries. The total experimental uncertainties $\delta\sigma_\gamma$ of the IRMM data are displayed on the top of each panel.

the data have been divided between panels (a), (b), and (c) in the figure. Panel (a) compares the various data sets from the threshold to $E_n = 2$ MeV. Panel (b) contains the results from experiments which have measurement points only for $E_n < 6$ MeV. Panel (c) compares our results with the data sets that cover high neutron energies. Finally, the IRMM data are plotted together with three evaluated libraries (ENDF/B-VII.1 [48], JEFF-3.1 [49], and JENDL-4.0 [50]) in panel (d). As can be seen from Fig. 5(a), from the inelastic threshold up to about $E_n = 0.8$ MeV there is good agreement between all data sets except that of Smith, which lies slightly lower, although with very large uncertainties in neutron energy. Above 0.8 MeV, the results of Freeman *et al.* and Dickens *et al.* also fall below the other data sets. At approximately 1 MeV, the IRMM values rise above the others, remaining fairly constant up to 1.4 MeV. Above 1.2 MeV, our results agree best with the data of Dickens *et al.* and Presser. As can be seen from panel (b), our results are consistently higher than all the others from approximately $E_n = 1$ MeV. The reasonable agreement with the IRMM data with those of Dickens *et al.* and Presser remains until approximately 4.5 MeV. After this until $E_n = 8$ MeV there is a good agreement between our results and those of Dickens *et al.* Above 8 MeV our data agrees well with those of Morgan. In Fig. 5(d), the total inelastic neutron scattering cross section from the evaluated libraries is compared with the IRMM data sets. The JENDL-4.0 evaluation is in a slightly better agreement than the others with our data.

As can be seen from Fig. 5(c), there are significant discrepancies between the IRMM data and the other sets having a large number of measurement points. As different methods for beam monitoring have been used in the experiments, a possibility of systematic errors is obvious. Indeed, [17] reports

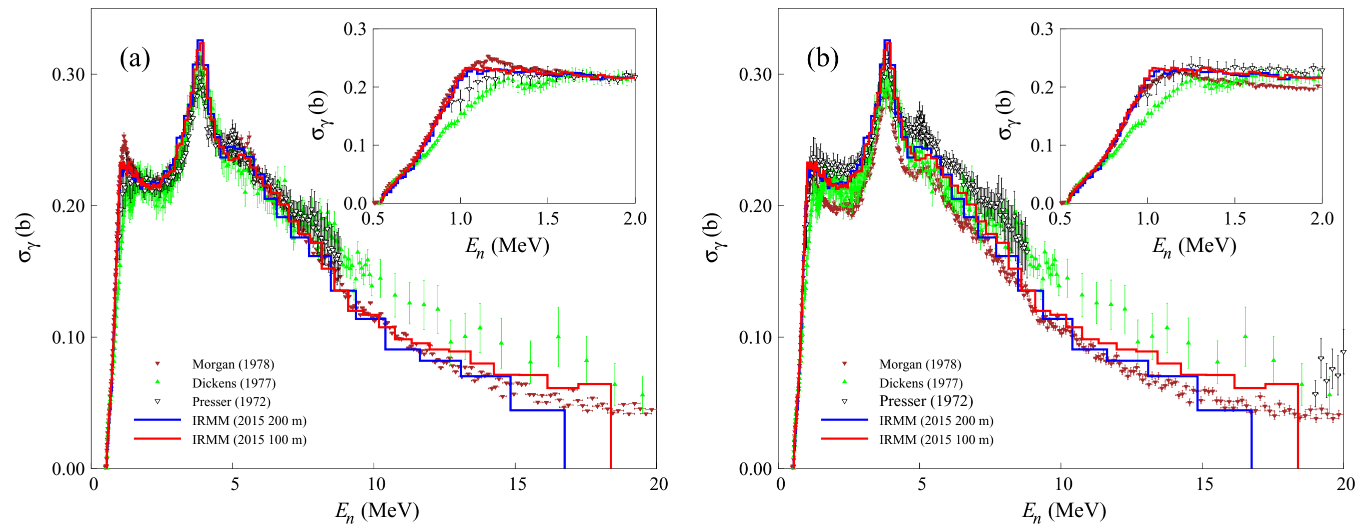

FIG. 6. (a) Cross section data of Presser and Bass, Morgan, and Dickens *et al.*, when normalized to converge with the IRMM data at a neutron energy of $E_n = 2$ MeV. (b) The unnormalized data provided for comparison. The low-energy region of the cross section is displayed in the insets.

an absolute cross-section scale uncertainty up to $\pm15\%$. In order to investigate the compatibility of the different data sets, those of Presser and Bass, Morgan, and Dickens *et al.* were normalized to converge with the IRMM data (100 m measurement) at three different neutron energies. The chosen normalization points were $E_n = 2$, $E_n = 5$, and $E_n = 8$ MeV. Both the 2- and 5-MeV normalizations produce a fairly good overall agreement (the 2-MeV one being the better of the two), but the 8-MeV normalization leads to large differences at lower energies. In Fig. 6(a), the 2-MeV normalization is displayed, with the unnormalized data provided for comparison in panel (b). In general our data agree best with those of Morgan, while the data set of Dickens *et al.* diverges from ours at high neutron energies regardless of the normalization chosen. The data of Dickens *et al.*, and to a lesser degree also those of Presser and Bass, behave differently than the others between 0.8 and 1.5 MeV, as can be seen from the inset of Fig. 6(a). The reason for this is not known, although in [24] it is mentioned that separate neutron-flux measurements were carried out for $E_n < 1$ and $E_n > 1$ MeV. Overall these comparisons indicate that, while systematic differences over the entire energy range can be reduced, discrepancies still remain.

B. CDCC calculations

Theoretical descriptions of inelastic neutron scattering on ^{6,7}Li have recently been published by Guo *et al.* [51], Ichinkhorloo *et al.* [52], and Matsumoto *et al.* [53]. All these studies employed the CDCC method with the complex Jeukenne-Lejeune-Mahaux (JLM) effective nucleon-nucleon interaction [54]. In [51], the experimental total neutron and proton scattering cross sections on ^{6,7}Li were used to determine energy-dependent normalization factors, which were then used to calculate the angular distributions of elastic and inelastic proton or neutron scattering. In all cases, a reasonably good agreement with experimental data was obtained. However, the inelastic neutron scattering cross section to the first excited state in ^{7}Li is not provided in [51,52]. Instead, the sum of elastic and inelastic scattering to the first excited state in the $n + {}^7$Li reaction, as well as the inelastic scattering to the second excited state at 4.63 MeV, are evaluated. Also no calculations are performed for $E_n < 4$ MeV.

Recently, the elastic neutron scattering cross section and the inelastic cross sections to the first and second excited states in ^{7}Li have been calculated by Ichinkhorloo *et al.* [55]. A comparison between the calculated ^{7}Li(n,n_1) cross section and the IRMM data is shown in Fig. 7. Above 7 MeV the agreement is good. At lower energies, the calculated results reproduce the general shape of the experimental cross-section curve fairly well; however, the calculated cross sections are lower than the experimental values and the theoretical curve appears shifted to higher neutron energies. For $E_n < 10$ MeV, the coupling potentials using the JLM interaction have not been constructed, necessitating the use of the optical model potential. Furthermore, for $2 < E_n < 5$ MeV, an independent

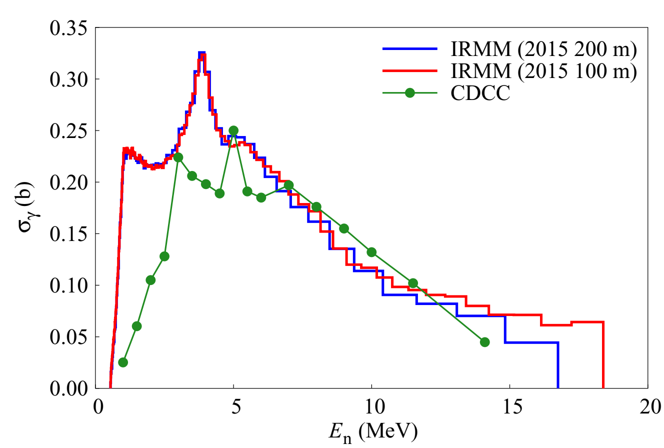

FIG. 7. Comparison between our experimental data and a recent calculation [55] using the CDCC method.

normalization was necessary. Above $E_n = 5$ MeV, the calculation used the same normalization for both elastic and inelastic cross sections. Clearly, there is still room for improvement in the CDCC calculations, especially at low energies.

V. SUMMARY

Neutron inelastic scattering by ^{7}Li was studied with the GAINS setup at the GELINA time-of-flight facility. The γ-ray production cross section for the 477.6-keV transition was measured from the threshold up to $E_n = 18$ MeV with a total relative uncertainty less than 5% for $1 < E_n < 8$ MeV. Comparisons were made between previous experimental data and the current results, and discrepancies were discussed. Additionally, results from recent CDCC calculations were provided, showing a reasonable agreement with the experimental data.

ACKNOWLEDGMENTS

We wish to thank the GELINA staff for the efficient operation of the accelerator. We also gratefully acknowledge the contributions of Y. Hirabayashi (Information Initiative Center, Hokkaido University), K. Katō, M. Aikawa (Nuclear Reaction Data Centre, Hokkaido University), and S. Chiba (Research Laboratory for Nuclear Reactors, Tokyo Institute of Technology) for their contributions to the CDCC calculations.

[1] A. D. Carlson, V. G. Pronyaev, R. Capote, F.-J. Hambsch, F. Käppeler, C. Lederer, W. Mannhart, A. Mengoni, R. O. Nelson, A. J. M. Plompen, P. Schillebeeckx, S. Simakov, P. Talou, S. Tagesen, H. Vonach, A. Vorobyev, and A. Wallner, Nucl. Data Sheets **118**, 126 (2014).
[2] A. D. Carlson, V. G. Pronyaev, R. Capote, G. M. Hale, F.-J. Hambsch, T. Kawano, S. Kunieda, W. Mannhart, R. O. Nelson, D. Neudecker, P. Schillebeeckx, S. Simakov, D. L. Smith, P. Talou, X. Tao, A. Wallner, and W. Wang, Nucl. Data Sheets **123**, 27 (2015).
[3] U.S. DOE Nuclear Energy Research Advisory Committee and the generation IV international forum (GIF): A technology roadmap for generation IV nuclear energy systems, https://www.gen-4.org/ (2002).
[4] J. M. Freeman, A. M. Lane, and B. Rose, Philos. Mag. **46**, 17 (1955).
[5] N. A. Bostrom, I. L. Morgan, J. T. Prud'homme, P. L. Okhuysen, and O. M. Hudson Jr., Neutron Interactions in Lithium, Carbon, Nitrogen, Aluminum, Argon, Manganese, Yttrium, Zirconium, Radiolead and Bismuth, Wright Air Development Center Report No. WADC-TN-59-10710, 1959 (unpublished).
[6] J. Benveniste, A. C. Mitchell, C. D. Schrader, and J. H. Zenger, Nucl. Phys. **38**, 300 (1962).
[7] J. Benveniste, A. C. Mitchell, C. D. Schrader, and J. H. Zenger, Nucl. Phys. **19**, 52 (1960).
[8] J. Benveniste, A. C. Mitchell, C. D. Schrader, and J. H. Zenger, Nucl. Phys. **19**, 448 (1960).
[9] N. P. Glazkov, J. Nucl. Energy, Parts A/B **18**, 656 (1964).
[10] R. Batchelor and J. H. Towle, Nucl. Phys. **47**, 385 (1963).
[11] J. C. Hopkins, D. M. Drake, and H. Condé, Nucl. Phys. A **107**, 139 (1968).
[12] H. H. Knitter and M. Coppola, in *Proceedings of the Conference on Neutron Cross Sections and Technology*, edited by D. T. Goldman (U.S. National Bureau of Standards, Washington, D.C., USA, 1968), Vol. II, pp. 827–836.
[13] N. P. Glazkov, Sov. At. Energy **14**, 405 (1964).
[14] J. H. Towle and W. B. Gilboy, Nucl. Phys. **32**, 610 (1962).
[15] H. Condé, D. M. Drake, and J. C. Hopkins, in *Proceedings of the Conference on Neutron Cross Section Technology* (Washington, D.C., 1966), AEC Report No. CONF-660303, p. 735.
[16] N. Ahmed, M. Coppola, and H.-H. Knitter, Measurements of Neutron Elastic Scattering from Carbon in the Energy Region of 0.50 to 2.00 MeV, Laboratory Report No. EUR4538e, Central Bureau for Nuclear Measurements (CBNM), 1970 (unpublished).
[17] G. Presser and R. Bass, Nucl. Phys. A **182**, 321 (1972).
[18] D. L. Smith, Nucl. Sci. Eng. **61**, 540 (1976).
[19] D. K. Olsen, G. L. Morgan, and J. W. McConnell, Nucl. Sci. Eng. **74**, 219 (1980).
[20] D. L. Smith, A Spectrometer for the Investigation of Gamma Radiation Produced by Neutron-Induced Reactions, Nuclear Data Measurements Report No. ANL/NDM-12, Argonne National Laboratory, 1975 (unpublished).
[21] D. L. Smith, Sample-Size Effects in Fast-Neutron Gamma-Ray Production Measurements: Solid-Cylinder Samples, Nuclear Data Measurements Report No. ANL/NDM-17, Argonne National Laboratory, 1975 (unpublished).
[22] D. L. Smith, Fast-Neutron Gamma-Ray Production from Elemental Iron: $E_n \leqslant 2$ MeV, Nuclear Data Measurements Report No. ANL/NDM-20, Argonne National Laboratory, 1976 (unpublished).
[23] G. L. Morgan, D. K. Olsen, and J. W. McConnell, Nucl. Instrum. Methods **157**, 525 (1978).
[24] J. K. Dickens, G. L. Morgan, G. T. Chapman, T. A. Love, E. Newman, and F. G. Perey, Nucl. Sci. Eng. **62**, 515 (1977).
[25] G. L. Morgan, Cross Sections for the ^{7}Li(n,xn) and ^{7}Li(n,n'γ) Reactions Between 1 and 20 MeV, Technical Memo No. ORNL-TM-6247, Oak Ridge National Laboratory, 1978 (unpublished).
[26] G. L. Morgan, T. A. Love, and F. G. Perey, Nucl. Instrum. Methods **128**, 125 (1975).
[27] V. M. Besotosnyj, V. M. Gorbachev, L. M. Suvorov, and M. S. Shvecov, Voprosy atomnoi nauki i techniki, ser. Yadernye Konstanty **19**, 77 (1975).
[28] H. D. Knox, R. O. Lane, D. A. Resler, and P. E. Koehler, in *Proceedings of the International Conference on Nuclear Cross Sections for Technology*, edited by J. L. Fowler, C. H. Johnson, and C. D. Bowman (U.S. National Bureau of Standards, Washington, D.C., USA, 1980), pp. 783–787.
[29] N. Otuka, E. Dupont, V. Semkova, B. Pritychenko, A. I. Blokhin, M. Aikawa, S. Babykina, M. Bossant, G. Chen, S. Dunaeva, R. A. Forrest, T. Fukahori, N. Furutachi, S. Ganesan, Z. Ge, O. O. Gritzay, M. Herman, S. Hlavač, K. Katō, B. Lalremruata *et al.*, Nucl. Data Sheets **120**, 272 (2014).
[30] H. D. Knox, R. M. White, and R. O. Lane, Nucl. Sci. Eng. **69**, 223 (1979).

[31] R. O. Lane, Study of Structure of Light Nuclei with Neutrons, Progress Report No. COO-2490-7, Ohio University, 1977 (unpublished).
[32] H. D. Knox and R. O. Lane, Nucl. Phys. A **359**, 131 (1981).
[33] H. D. Knox, D. A. Resler, and R. O. Lane, Nucl. Phys. A **466**, 245 (1987).
[34] M. Kamimura, M. Yahiro, Y. Iseri, Y. Sakuragi, H. Kameyama, and M. Kawai, Prog. Theor. Phys. Suppl. **89**, 1 (1986).
[35] N. Austern, Y. Iseri, M. Kamimura, M. Kawai, G. Rawitscher, and M. Yahiro, Phys. Rep. **154**, 125 (1987).
[36] L. C. Mihailescu, L. Oláh, C. Borcea, and A. J. M. Plompen, Nucl. Instrum. Methods Phys. Res., Sect. A **531**, 375 (2004).
[37] C. Theis, K. H. Buchegger, M. Brugger, D. Forkel-Wirth, S. Roesler, and H. Vincke, Nucl. Instrum. Methods Phys. Res., Sect. A **562**, 827 (2006).
[38] A. Plompen, N. Nankov, C. Rouki, M. Stanoiu, C. Borcea, D. Deleanu, A. Negret, P. Dessagne, M. Kerveno, G. Rudolf, J. C. Thiry, M. Mosconi, and R. Nolte, J. Korean Phys. Soc. **59**, 1581 (2011).
[39] C. Rouki, P. Archier, C. Borcea, C. De Saint Jean, J. C. Drohé, S. Kopecky, A. Moens, N. Nankov, A. Negret, G. Noguère, A. J. M. Plompen, and M. Stanoiu, Nucl. Instrum. Methods Phys. Res., Sect. A **672**, 82 (2012).
[40] L. C. Mihailescu, C. Borcea, and A. J. M. Plompen, Nucl. Instrum. Methods Phys. Res., Sect. A **578**, 298 (2007).
[41] K. J. R. Rosman and P. D. P. Taylor, Pure Appl. Chem. **70**, 217 (1998).
[42] A. D. Carlson, V. G. Pronyaev, D. L. Smith, N. M. Larson, Z. Chen, G. M. Hale, F.-J. Hambsch, E. V. Gai, S.-Y. Oh, S. A. Badikov, T. Kawano, H. M. Hofmann, H. Vonach, and S. Tagesen, Nucl. Data Sheets **110**, 3215 (2009), Special Issue on Nuclear Reaction Data.
[43] G. Audi, A. H. Wapstra, and C. Thibault, Nucl. Phys. A **729**, 337 (2003), The 2003 NUBASE and Atomic Mass Evaluations.
[44] S. Nagy, T. Fritioff, M. Suhonen, R. Schuch, K. Blaum, M. Björkhage, and I. Bergström, Phys. Rev. Lett. **96**, 163004 (2006).
[45] D. Deleanu, C. Borcea, P. Dessagne, M. Kerveno, A. Negret, A. J. M. Plompen, and J. C. Thiry, Nucl. Instrum. Methods Phys. Res., Sect. A **624**, 130 (2010).
[46] X-5 Monte Carlo Team, *MCNP - A General N-Particle Transport Code*, Version 5, Volume I: Overview and Theory (Los Alamos National Laboratory, Los Alamos, New Mexico, USA, 2003, revised 2005).
[47] D. R. Tilley, H. R. Weller, C. M. Cheves, and R. M. Chasteler, Nucl. Phys. A **595**, 1 (1995).
[48] M. B. Chadwick, M. Herman, P. Obložinský, M. E. Dunn, Y. Danon, A. C. Kahler, D. L. Smith, B. Pritychenko, G. Arbanas, R. Arcilla, R. Brewer, D. A. Brown, R. Capote, A. D. Carlson, Y. S. Cho, H. Derrien, K. Guber, G. M. Hale, S. Hoblit, S. Holloway *et al.*, Nucl. Data Sheets **112**, 2887 (2011), Special Issue on ENDF/B-VII.1 Library.
[49] A. Santamarina, D. Bernard, P. Blaise, M. Coste, A. Courcelle, T. D. Huynh, C. Jouanne, P. Leconte, O. Litaize, S. Mengelle, G. Noguère, J.-M. Ruggiéri, O. Sérot, J. Tommasi, C. Vaglio, and J.-F. Vidal, *The JEFF-3.1.1 Nuclear Data Library*, JEFF Report No. 22 (OECD Nuclear Energy Agency, Issy-les-Moulineaux, France, 2009).
[50] K. Shibata, O. Iwamoto, T. Nakagawa, N. Iwamoto, A. Ichihara, S. Kunieda, S. Chiba, K. Furutaka, N. Otuka, T. Ohsawa, T. Murata, H. Matsunobu, A. Zukeran, S. Kamada, and J. Katakura, J. Nucl. Sci. Technol. **48**, 1 (2011).
[51] H. Guo, Y. Watanabe, T. Matsumoto, K. Ogata, and M. Yahiro, Phys. Rev. C **87**, 024610 (2013).
[52] D. Ichinkhorloo, Y. Hirabayashi, K. Katō, M. Aikawa, T. Matsumoto, and S. Chiba, Phys. Rev. C **86**, 064604 (2012).
[53] T. Matsumoto, D. Ichinkhorloo, Y. Hirabayashi, K. Katō, and S. Chiba, Phys. Rev. C **83**, 064611 (2011).
[54] J.-P. Jeukenne, A. Lejeune, and C. Mahaux, Phys. Rev. C **16**, 80 (1977).
[55] D. Ichinkhorloo, M. Aikawa, S. Chiba, Y. Hirabayashi, and K. Katō (unpublished).